MAXI-SSC Results In 7 Years

Hiroshi Tsunemi,[1] Hiroshi Tomida,[2] Satoshi Nakahira,[3] and SSC team

[1] Department of Earth and Space Science, Osaka University,
1-1 Machikaneyama, Toyonaka, Osaka 560-0043 Japan
[2] Institute of Space and Astronautical Science, Japan Aerospace Exploration Agency,
3-1-1 Yoshinodai, Chuo, Sagamihara, kanagawa, 252-5210 Japan
[3] Human Spaceflight Technology Directorate, Japan Aerospace Exploration Agency,
2-1-1 Sengen, Tsukuba, Ibaraki, 305-805 Japan
E-mail(HT): tsunemi@ess.sci.osaka-u.ac.jp

Abstract

The MAXI SSC is a slit-camera using X-ray CCDs. Its field of view is $1° \times 90°$ and covers the whole sky. The CCD performance gradually degrades due to the charged particles while it has been working since its launch in 2009. Due to the small effective area of the slit, the SSC detection limit is higher than that of the MAXI GSC whereas its effective energy range is between 0.6 keV and 7 keV. We have observed both point sources and diffuse emission. We will briefly review the SSC performance and its results in this 7 years.

Key words: instruments: X-ray CCDs — surveys — X-rays:general

1. SSC performance in orbit

The SSC is an X-ray slit-camera on board the MAXI (Matsuoka et al., 2009) launched in 2009 (Tsunemi et al., 2010, Tomida et al., 2011). It consists of two identical cameras, SSC-H and SSC-Z, looking at a horizontal direction and a zenith direction, respectively. Each camera contains 16 CCDs just below the mechanical slit that limits the field of view (FOV) of the SSC to be $1° \times 90°$. CCD functions in parallel sum mode as one dimensional imager. Each CCD has its own single-stage peltier cooler with which it is cooled below -60°C when the camera body is around -15°C. The peltier cooler achieves more than 40°C temperature difference by using 1 A electric current. The SSC camera body is connected to two radiators through a loop heat pipe. The surface of the radiators is painted in white so as to avoid to be too shinny.

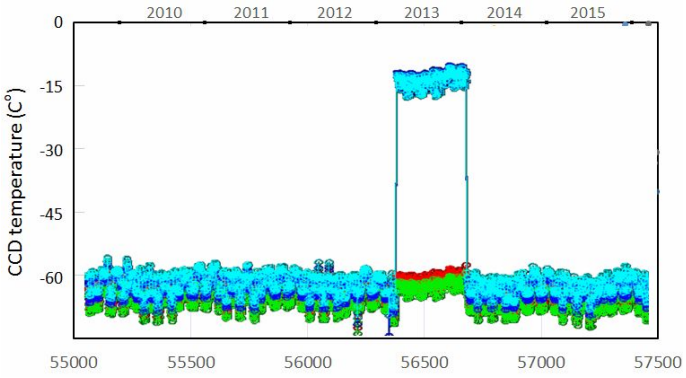

Fig. 1. Thermal history of the CCDs on the SSC in 7 years. SSC-Z was out of order in 2013 when the CCD temperature is that of the camera body temperature.

Figure 1 shows the thermal history of the CCD for 7 years. Almost all the CCDs are kept around -60°C with almost no degradation in cooling system. We had a CPU trouble in 2013 where SSC-Z was out of control for almost one year. During this period, CCDs in SSC-H were kept in cold condition while those in SSC-Z were left with no peltier cooling.

Each SSC camera receives Cu-K fluorescence lines in each CCD. Cu-K lines are generated by charged particles onto the slats collimator made of copper. We can monitor the performance of the CCD by measuring the standard deviation of the line profile. Figure 2 shows the evolution of the SSC performance for 7 years. We see that the SSC gradually degrades due to the charged particles. The degradation depends on the geometrical condition inside the SSC. The far-end of the CCD received a least damage while that just below the slit received the biggest damage. We should note that the SSC-Z in 2013 showed almost no degradation when its CCDs were left unbiased at around -15°C.

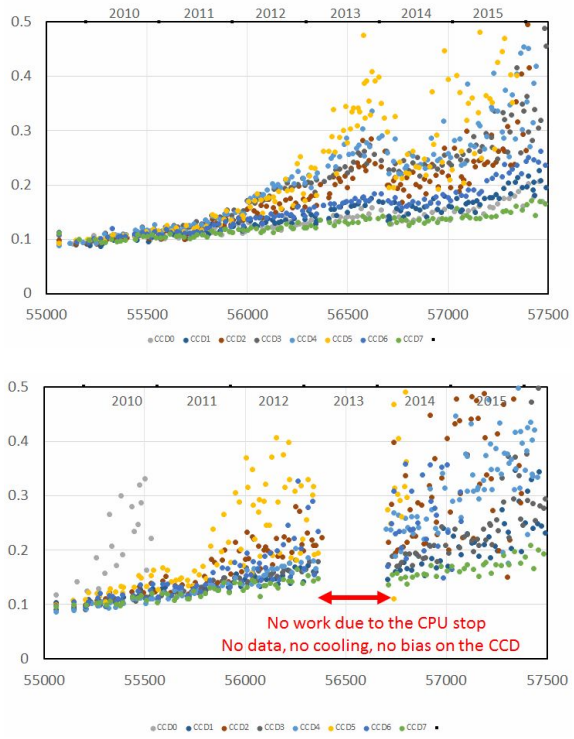

Fig. 2. Evolution of the CCDs on the SSC-H (top figure) and on the SSC-Z (bottom figure). The Cu-K line profile (standard deviation) is shown as a function of time.

The CCDs of the SSC are designed to be sensitive to X-rays while they are insensitive to visible photons by Al coat on the imaging area. However, we find that they are sensitive to infra-red, particularly at device edges. The data obtained at daytime are heavily saturated depending on the sun direction. Therefore, we usually collect data obtained at night time. This reduces the observation efficiency of the SSC by a factor of two.

2. Comparison with ROSAT

2.1. Point source observation

The SSC can cover the energy range between 0.6 and 7 keV. The low energy limit is determined by the thermal noise while the high energy limit is practically determined by the Cu-K lines. Tomida et al. (2016) generated the point source catalog using the SSC data between 2010 August to 2014 April and listed 170 sources. They measured the source intensity below and above 1.85 keV (soft band and hard band, respectively). The soft band is out of the GSC energy range (Mihara et al., 2011). There are 32 sources only seen in the soft band while other 30 sources are seen only in the hard band. The soft band data are the unique measurement of the entire sky since the ROSAT all sky survey in 1991 (Voges et al., 1999). Figure 3 shows the intensity correlation between the sources in SSC in soft band and those in ROSAT (0.1-2.4 keV). We see that there is a very clear correlation between them. Some sources, Cygnus X-1, Her X-1 etc. showing strong time variability deviate from a simple correlation. We also find that the detection limit of the SSC is a few mCrab.

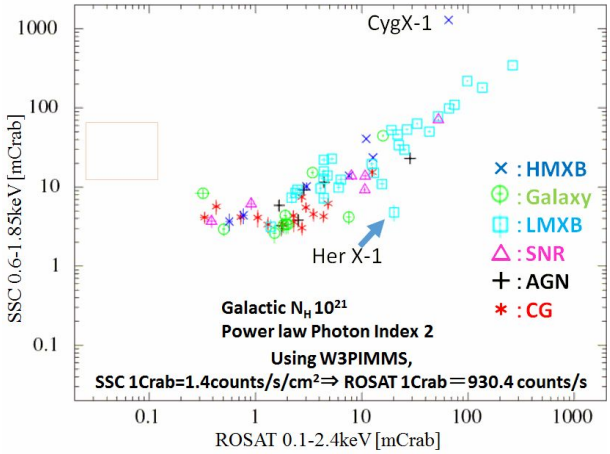

Fig. 3. Intensity correlation between point sources detected by the SSC and those by ROSAT. Some sources show intensity change in this 20 years.

2.2. Diffuse structure in the entire sky

The SSC covers the entire sky in unbiased scan observation. Since its energy range is below 2 keV, this is also a unique sky map since the ROSAT all sky survey in 1991 (Freyberg et al., 1999). Figure 4 shows the comparison of the sky map between the SSC (0.6-1.0 keV) and the ROSAT (0.44-1.21 keV). In both maps, bright point sources are eliminated so that the we can see a diffuse emission structure in detail. The angular resolution of the SSC is about a few degrees while that of ROSAT is about an order of magnitude better. We see that they are quite similar to each other with taking into account the difference in angular resolution.

3. GRB Nova and CSB

3.1. GRB

The SSC scans the sky in the fan beam according to the orbital motion of the International Space Station orbital motion. Therefore, a typical on-source time is about 50 seconds at every 90 minutes. We have detected several short-time transients under this circumstance. Among them, we detected the initial phase of GRB100418A from its very beginning (Imatani et al., 2016). Some GRBs having a pre-cursor were detected by the BAT. The following observation by the Swift/XRT could cover the main part of it (Romano, et al., 2006). While many of them show no pre-cursor whose main peak is difficult to be observed from its beginning.

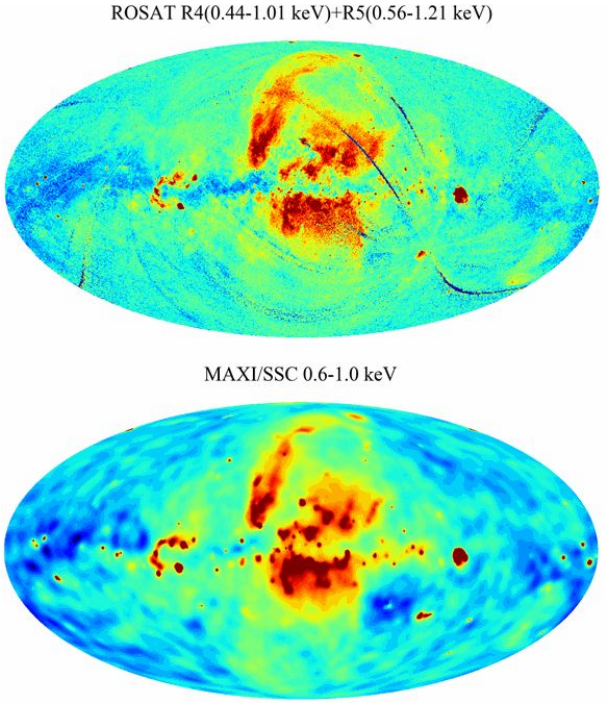

Fig. 4. Comparison of the SSC diffuse map with that of ROSAT. With taking into account the difference in spatial resolution, we see that they are identical to each other.

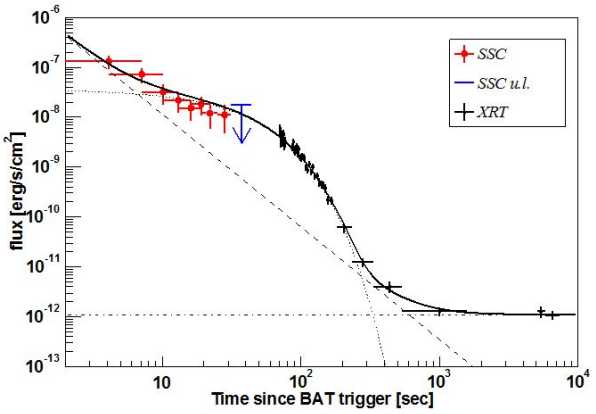

Fig. 5. Entire light curve of GRB100418B. The first 50 second was observed by the SSC and followed by the Swift/XRT.

Figure 5 shows the light curve of GRB100418A. It was a typical long GRB. When the source entered the FOV of the SSC, the GRB started that was detected by the BAT on Swift. It reached a maximum flux of a few ten times brighter than that of the Crab nebula. The SSC monitored its light curve for the initial 50 seconds. The Swift/XRT pointed to the source 71 second after its emergence (Marshall, et al., 2011).

The light curve of the GRB can be well expressed by a power law of time. By adding the SSC data in the prompt emission, we found that the light curve could be expressed not by a power law but by a combination of a power law and an exponential component of a decay time about 30 second. In the first 300 second, the exponential components dominates the emission. We found that GRB100418A is a typical long GRB having a very low value of Ep($\leq$ 8.3 keV) that is a very rare GRB. It is also consistent with the Yonetoku-relation (Yonetoku et al., 2010) while it is marginal with the Amati-relation (Amati et al., 2008).

3.2. Nova

MAXI detected many transients including nova. Since the GSC has much better detection efficiency, the SSC can confirm it if it is bright enough. A MAXI nova, MAXI J0158−744, was discovered in the SMC by the GSC in 2011. The SSC followed the observation about 20 minutes after. It was still bright and we obtained the X-ray spectrum where we detected the emission lines from Ne and Mg (Morii et al., 2013) showing the thin thermal origin.

We confirmed that the transient is a nova explosion, on a white dwarf in a binary with a Be star. An early turn-on of the super-soft X-ray source (SSS) phase, the short SSS phase duration of about one month, and a 0.92 keV Ne emission line found in the third MAXI scan, suggest that the explosion involves a small amount of ejecta and is produced on an unusually massive O-Ne white dwarf close to, or possibly over, the Chandrasekhar limit. We propose that the huge luminosity detected with MAXI is due to the fireball phase, a direct manifestation of the ignition of the thermonuclear runaway process in a nova explosion.

3.3. Cygnus Super Bubble

There are several large scale structures in soft X-ray band as shown in figure 4. One of them is the Cygnus Super Bubble (CSB) that is well-known discovered by HEAO-1 in 1980 (Cash, et al., 1980) and ROSAT also confirmed it. These observations were done by using a gas proportional counter which was difficult to reveal its spectral origin. Figure 6 shows the SSC map around the CSB where there are 3 Cygnus point sources and the Cygnus Loop. The CSB is an extended source of about 15° × 25°.

We detected emission lines of Ne and Mg as shown in figure 7 which confirms a thin thermal origin rather than a non-thermal origin. The temperature is about 0.23±0.01 keV with a depleted abundance of 0.26±0.1 solar. The abundance depletion is also known in the Cygnus Loop (Miyata et al., 1994) that is close to the CSB. It may reflect the interstellar matter in this region. By adding the ROSAT data at low energy, we also confirm that the interstellar absorption feature shows no variation within the uncertainties suggesting that the

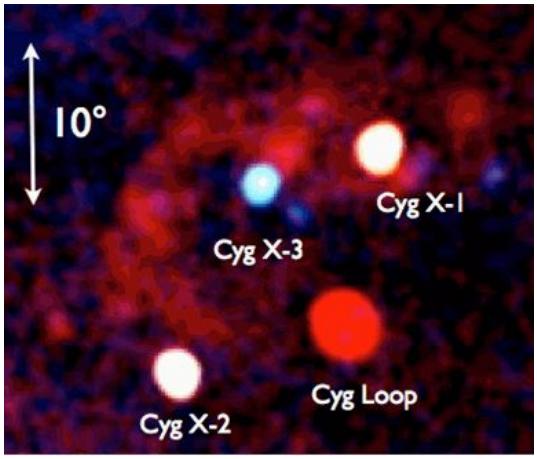

Fig. 6. CSB image in the Cygnus region. There are three points sources (Cyg X-1, X-2 and X-3) and the Cygnus Loop.

CSB is a single unity. The Cygnus OB2 association is difficult to be an energy source, since it is off-centered of the CSB. With taking into account the total thermal energy, we conclude that it can originate from a hypernova event rather than a rapid sequence of many supernovae (Kimura et al., 2013).

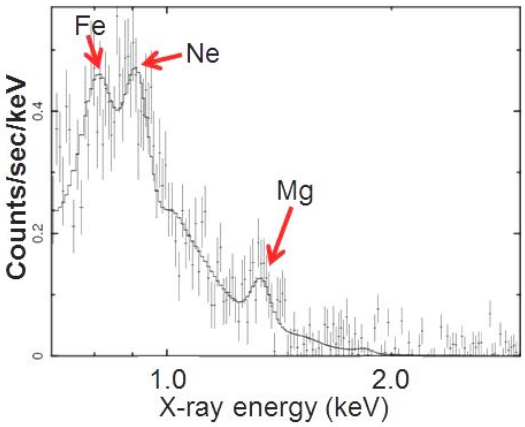

Fig. 7. X-ray spectrum of the CSB. It can be well expressed by a thin thermal origin with a depleted abundance.

4. Diffuse structure and Fermi bubble

Figure 8 shows the SSC sky maps in three energy bands: 0.6-1 keV, 1-2 keV and 2-4 keV. The 2-4 keV band map shows many point sources as well as the galactic ridge emission that is clearly seen in the GSC map. The 0.6-1 keV map shows diffuse emission in large structure.

Figure 9 shows the SSC color map where red, green and blue correspond to those of three bands in figure 8. We see that low energy diffuse structures are seen in red, while point sources along the galactic plane are seen in

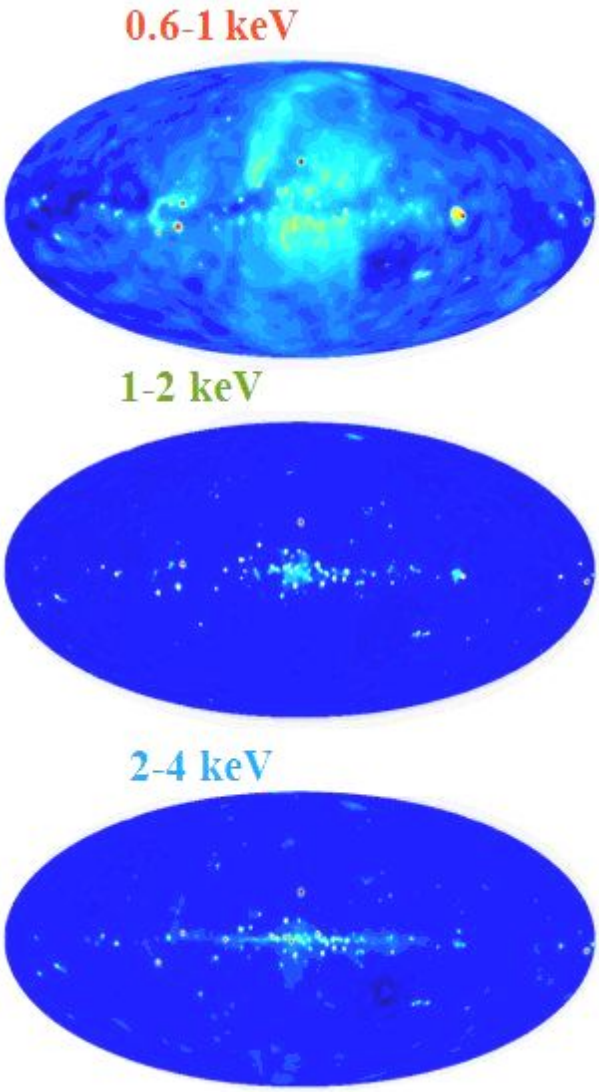

Fig. 8. SSC band map images of the whole sky

blue. The most prominent large structure is seen in the galactic center. We see that there is a large structure in the northern hemisphere, emerging from the galactic plane along the North Polar Spur and reaches near the north pole and goes down to the galactic plane. We also see the structure in the south hemisphere that is quite compact to that seen in the north. It clearly shows asymmetry in the north and south structure and clearly off-set from the galactic center.

A giant gamma-ray structure was discovered by Fermi in the energy range of 1-10 GeV (Dobler et al., 2010). They reported that a feature emerges from the galactic center and extends 50° north and south from the plane of the Milky Way, forming a dumbbell shape. This suggests an explosion from the galactic center. There are several reports that the X-ray feature is connected with

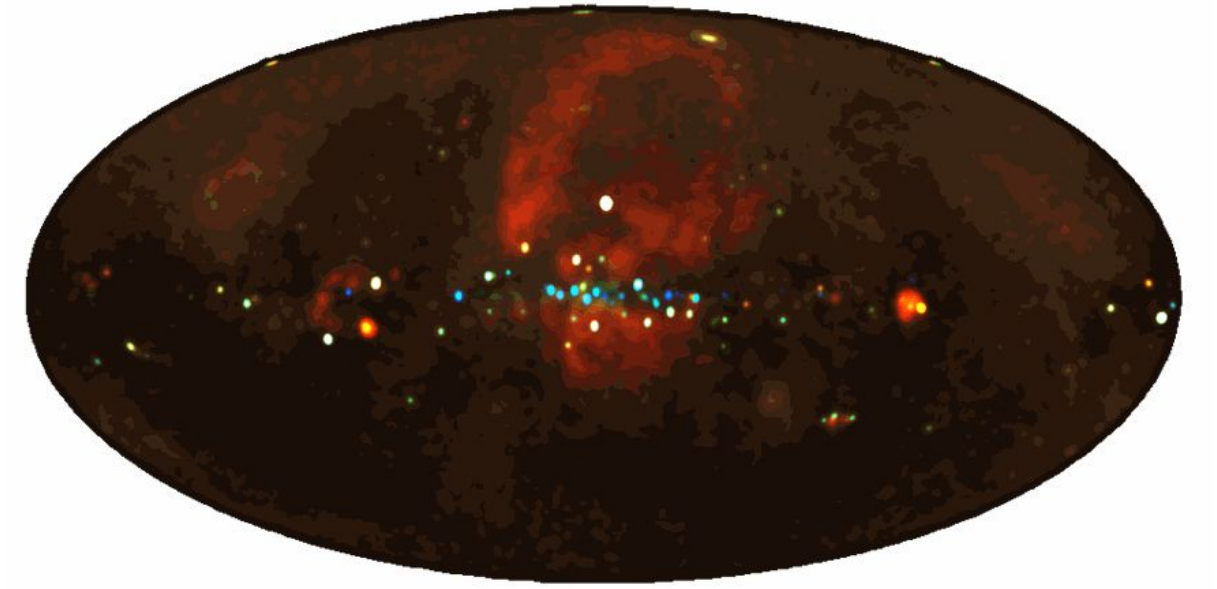

Fig. 9. SSC color map of the entire sky where red, green and blue correspond to the energy ranges of 0.6-1 keV, 1-2 keV and 2-4 keV.

the Fermi bubble. Kataoka, et al. (2013) performed observation using Suzaku. Since it has a relatively small FOV, of 22′ square, they observed several points around the edge of the Fermi bubble, north and south. They detected an intensity or temperature jump at the edge location they selected. The spectrum reported is in thermal origin, rather than non-thermal origin.

Comparing the Fermi bubble map with that of the SSC, we see that there is not so clear correlation between them. In the north hemisphere, the Fermi bubble corresponds to the relatively weak emission in X-ray. The X-ray feature seems to surround the Fermi bubble, suggesting the formation of the shock front. In the south hemisphere, however, the Fermi bubble surely includes the X-ray bright region.

We have accumulated the spectrum from the extended region covering the Fermi bubble shown in figure 10. We find that it can not be non-thermal origin. Although we have to modify the abundance for Ne and Mg, it is a thin thermal origin. This result is consistent with that by the Suzaku observation (Kataoka et al., 2013), although Suzaku observed a very small region.

Then, we divide the X-ray structure into several segments; inside the Fermi bubble, outside the Fermi bubble, north, south according by latitude and longitude. We find that the plasma temperature is almost constant, 0.31 keV whole through the region. The absorption feature, $N_{\rm H}$, is a reliable distance indicator in X-ray. However, we can not determine $N_{\rm H}$ due to the fact that our data are insensitive below 0.6 keV. According to the ROSAT data, there is an intensity variation at low energy due to the local hot bubble or the solar wind charge

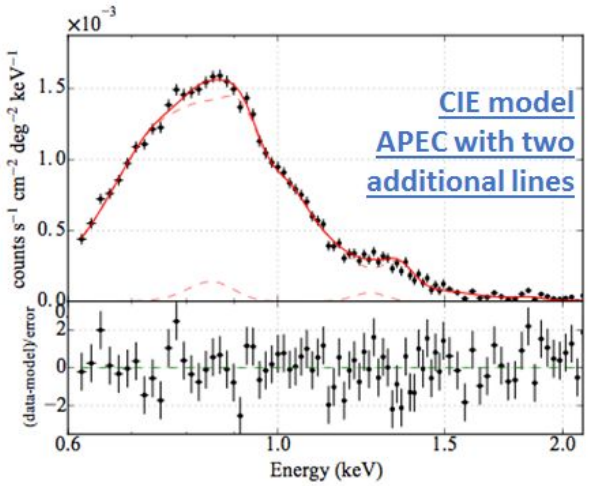

Fig. 10. SSC spectrum around the Fermi bubble region

exchange or whatever. It will be quite difficult to estimate the value of $N_{\rm H}$ even if we are sensitive to low energy. We need higher energy resolution below 0.6 keV.

Figure 11 shows a simple sphere projection using JUDO2 (http://www.darts.isas.jaxa.jp/astro/judo2/). The figure center is selected by the center of the X-ray structure so that almost all the extended emission can be easily seen here. It is about 20° away from the galactic center and not on the galactic plane. There are many galactic sources along the galactic plane where they contaminate the extended emission. Apart from them, we see that the soft X-ray emission is well within a circle with a radius of 50°. The north polar spur is

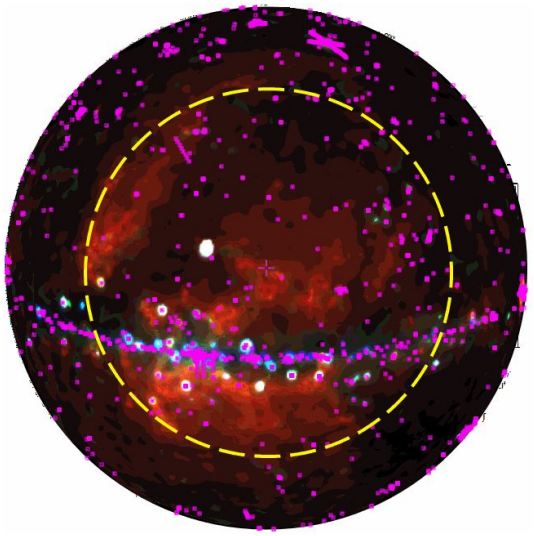

Fig. 11. Diffuse structure around the Fermi bubble region

relatively bright in the north-east edge. Other than that, it reminds us a center-filled SNR with a large scale. Pink color spots in figure 11 indicate the FOV of the Suzaku observations performed so far, most of them are for the specific point sources. Very few are for the study of the extended structure (Kataoka et al., 2013). They can cover much less than 1% of the X-ray large structure. We have measured the average emission integral (EI) of the large structure along the line of sight. We find EI 1 $\sim 4 \times 10^{-2}\mathrm{cm}^{-6}\,\mathrm{pc}$ with which we can estimate the total mass (M_{t}) and the thermal energy (E_{th}) as below, where D is the distance to the source and kT is the temperature.

$$M_{\mathrm{t}} \sim 6 \times 10^{4} (\frac{D}{1\,\mathrm{kpc}})^{2.5}\, M_{\odot}$$

$$E_{\mathrm{th}} \sim 4 \times 10^{52} \frac{\mathrm{kT}}{0.3\,\mathrm{keV}} (\frac{D}{1\,\mathrm{kpc}})^{2.5} \mathrm{erg}$$

The X-ray structure showing circular shape is off-set from the galactic center while the Fermi bubble is symmetry on the galactic center. In the northern hemisphere, the X-ray bright region surrounds the Fermi bubble while in the southern hemisphere, the X-ray bright region is surrounded by the Fermi bubble. This suggests that they are accidentally seen in the same line of sight. If the X-ray structure originates from the galactic center, M_{t} is an order of $10^{7}\mathrm{M}_{\odot}$ and E_{th} is an order of 10^{55}erg. This requires us a very strong AGN activity in our galaxy. If the source is well within one kpc, these two values become plausible, supplied by hypernova or a series of supernova. The precise distance determination is the key to solve this problem. The observation below 0.6 keV using good energy resolution will be able to determine the value of N_{H} to decide whether the X-ray structure is around the galactic center or is very close to us. We expect that the near future observation with eROSITA (http://www.mpe.mpg.de/eROSITA) will solve this problem.

The SSC operation is supported by many people in the MAXI team as well as students who work outside the team at present. We greatly appreciate all the efforts they have done so far.

References

Amati, L., et al., 2008, MNRAS, 391, 577
Cash, W., et al. 1980 ApJ., 238, L71
Dobler, G., 2010, ApJ., 717, 825
Freyberg, M. J., et al., 1999, HXRA conf. 278
Imatani, R., et al. 2016 PASJ., 68, S19
Kataoka, J., et al. 2013 ApJ., 779, 57
Kimura, M., et al. 2013 PASJ., 65-1, 14
Marshall, F. E. et al. 2011 ApJ., 727, 132
Matsuoka, M., et al., 2009 PASJ., 61, 999
Mihara, T., et al., 2011 PASJ., 63S, 623
Miyata, E., et al., 1994 PASJ., 46L, 101
Morii, M., et al. 2013 ApJ., 779, 118
Romano, P., et al. 2006 A&A, 456, 917
Tomida, H., et al. 2011 PASJ., 63, 397
Tomida, H., et al. 2016 PASJ., 68, S32
Tsunemi, H., et al. 2010 PASJ., 62, 1371
Voges, W., et al. 1999 A& A, 349, 389
Yonetoku, E., et al., 2010 PASJ, 62, 1495